Chapter 15
Development and Validation of a Novel Miniaturized High-Precision Laser Vibrometer for Vibration and Ultrasonic Vibration Measurements

Ke Yuan, Zhonghua Zhu, Wei Chen, and Weidong Zhu

Abstract Developing a miniatured laser vibrometer becomes important for many engineering areas, such as experimental and operational modal analyses, model validation, and structural health monitoring. Due to its compact size and light weight, a miniatured laser vibrometer can be attached to various mobilized platforms, such as an unmanned aerial vehicle and a robotic arm whose payloads can usually not be large, to achieve a flexible vibration measurement capability. However, integrating optics into a miniaturized laser vibrometer presents several challenges. These include signal interference from ghost return signals generated by sub-components of integrated photonics, polarization effects caused by waveguide structures, and wavelength drifting due to the semiconductor laser, and poorer noise characteristics of an integrated laser chip compared to a non-integrated circuit. This work proposes a novel chip-based high-precision laser vibrometer by incorporating two or more sets of quadrature demodulation networks into its design. An additional set of quadrature demodulation networks with a distinct reference arm delay line length can be used to conduct real-time compensation to mitigate linear interference caused by temperature and environmental variations. A series of vibration measurements with frequencies ranging from 0.1 Hz to 1 MHz were conducted using the proposed laser vibrometer to show its repeatability and accuracy in vibration and ultrasonic vibration measurements, and its robustness to test surface conditions. The proposed laser vibrometer has the advantage of directly measuring the displacement response of a vibrating structure rather than integrating its velocity response to yield the measured displacement with a laser Doppler vibrometer.

Keywords Miniatured laser vibrometer · Integrated optics · Quadrature demodulation network · Vibration measurement · Ultrasonic vibration measurements

Introduction

A laser Doppler vibrometer (LDV) can measure the velocity response of a vibrating structure based on the Doppler shift principle. As a noncontact vibration measurement device, it can avoid mass loading and is more suitable than a contact-type device, such as an accelerometer and a linear variable differential transducer, for measuring vibration of a light-weight and fragile structure. Scanning LDV and continuously scanning LDV techniques were developed to make LDV measurements automated, rapid, and dense. Experimental and operational modal analyses using a LDV have been widely used in engineering areas, such as model validation, modal identification, structural health monitoring, and damage detection of beams [1], plates [2], pipes [3, 4], bridges [5, 6], buildings [7, 8], turbine blades [9, 10], and sandwich structures [11, 12].

With the development of unmanned system techniques, attaching a LDV on an unmanned system, such as an unmanned aerial vehicle (UAV) [13, 14] and a robotic arm [15–18], for vibration measurement becomes more and more popular. By taking the LDV off a tripod, which provides a common support for the LDV, vibration measurement can be more flexible and practical. However, for such UAV+LDV and Robot+LDV systems, one of major challenges was limitations of payloads

Ke Yuan · Weidong Zhu
Department of Mechanical Engineering, University of Maryland Baltimore County, Baltimore, MD 21250
e-mail: kyuan1@umbc.edu

Zhonghua Zhu · Wei Chen
OmniSensing Photonics, LLC, Columbia, MD 21046
e-mail: zhonghua.zhu@osphotonics.com; wei.chen@osphotonics.com

Janko Slavic et al. (eds.), *Computer Vision & Laser Vibrometry, Vol. 6*, Conference Proceedings
of the Society for Experimental Mechanics Series, https://doi.org/10.13052/97887-438-0151-1_15

of the UAV and the robot, as higher payloads indicated higher costs and risks during operations. In Ref. [14], the UAV with a sufficiently large payload was selected to hold both the sensor head and the LDV module. In most of the above Robot+LDV systems, industrial robotic arms were used to hold one or multiple laser heads, which needed large spaces for operation and were not practical for most laboratory scenarios. Other possible solutions for reducing robot payloads included separating a laser head and its accessories such as a laser excitation device [17], and using a LDV with a sufficiently small size.

This work aims at developing a new type of miniatured displacement-based laser vibrometers based on integrated optics to resolve the payload limitation issue. Most recent LDVs are designed using discrete optical components. The difference between discrete and integrated optical designs in LDVs can be compared to the difference between vacuum tube circuit and integrated circuit technologies in the electronics world. Main compact LDV techniques include photonic integrated circuits (PIC), laser feedback interferometry, and micro-machined free-space optical interferometers [19–21]. Ref. [20] presented a design on silicon-on-insulator (SOI) for measuring small vibrations at low frequencies. Integrated optics can put an entire optical system into a single chip to reduce its size and weight by thousands of times.

To address above limitations and challenges, this work proposes a novel chip-based high-precision laser vibrometer by incorporating two or more additional sets of quadrature demodulation networks into its design. Major contributions of this work include: (1) an additional set of quadrature demodulation networks with a distinct reference arm delay line length that can mitigate nonlinear interference caused by temperature and environmental variations by conducting real-time compensation; (2) the proposed laser vibrometer can directly measure the vibration displacement of a structure using a phase demodulation method, which is different from a frequency demodulation method used for a conventional LDV, which directly measures the vibration velocity and integrates it to obtain the displacement; and (3) the proposed laser vibrometer has good robustness to test surface conditions.

Working Principles Used in This Work

A laser Doppler vibrometer is developed based on working principles of laser interferometry. A simplified schematic diagram of a typical laser interferometer is shown in Figure 1. A laser diode (LD) with a narrow linewidth is usually preferred as the light source to ensure laser coherence and low phase noise, and a LD stabilizer unit can be used to stabilize its frequency. A beamsplitter is used to divide the laser beam into two: one as the measurement beam and the other as the reference beam. The measurement beam, after reflecting from a device under test (DUT), recombines with the reference beam to generate a beating signal that can be received by a photodetector (PD). Based on the relation between the frequency of the measurement beam and that of the reference beam, laser interferometers can be categorized as homodyne laser interferometers and heterodyne laser interferometers. In a homodyne laser interferometer, the two laser beams have the same frequency, and the displacement of the DUT can be obtained by analyzing the frequency or the phase shift of the beating signal. In a heterodyne laser interferometer, the two laser beams have different frequencies, which can be implemented by using a birefringence-Zeeman dual frequency laser as the laser source or by introducing an acousto-optic modulator (AOM) into its reference arm, as shown in the dashed box in Figure 1. Response of the DUT can then be obtained by analyzing the frequency or the phase shift of the beating signal. The beating signal with a high frequency, which is typically in the range of MHz, can effectively isolate measured response of the DUT from environmental noise to preserve measurement precision even in sub-optimal conditions. Heterodyne interferometers move signal frequencies to the MHz range while homodyne interferometers have signal frequencies to remain at original frequencies, which results in the fact that heterodyne interferometers are less susceptible to low frequency noises than homodyne interferometers. There are several low frequency noises. One is the $1/f$ noise, where f is the driver frequency, from electronics that typically affects the LD driver and causes a high signal noise level in the low frequency range. Also, optical components are susceptible to temperature change, which is usually slow and becomes another major noise source in the low frequency range. Consequently, heterodyne interferometers have a better noise performance. Therefore, strong resistance to environmental noise is one of major advantages of a heterodyne laser interferometer over a homodyne laser interferometer whose reference optical path is susceptible to environmental disruption in a non-integrated setting.

There are two methods to demodulate the vibration signal received by the PD. The first one is the phase demodulation method. It employs demodulation of amplitude changes of the received signal or filtering to directly obtain the envelope of the signal, thereby extracting changes of the signal phase. The second one is the frequency demodulation method. Devices such as lock-in amplifiers can accurately detect changes in the frequency of the signal. Frequency shifts indicate changes in the physical quantity being measured. However, in this configuration, PD loses the complex signal information carried by photons in converting the received light power into the electrical signal. The most straightforward benefit of a complex baseband architecture is the noise-figure improvement achievable by eliminating the imaginary band noise foldback. In the-

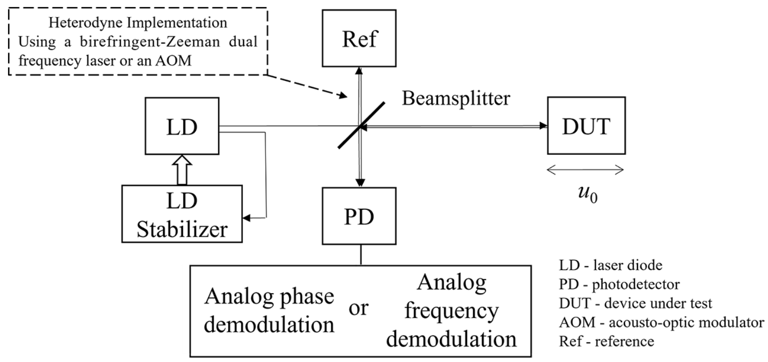

Fig. 1 schematic diagram of a laser interferometer: the homodyne configuration without heterodyne implementation marked by the dashed box, and the heterodyne configuration.

ory, the noise-figure improvement is 3 dB [22]. Environmental changes, mainly the thermal effect, result in design parameter variations of various optical components, especially for an integrated photonic chip. With a complex domain signal, these changes can be compensated in digital decoding [23]. Therefore, the amplitude signal is highly susceptible to system noise and environmental noise. The frequency demodulation method is more precise under conditions with low signal-to-noise ratios (SNRs), and most commercial laser vibrometers are essentially heterodyne laser interferometers using the frequency demodulation method, earning them the name LDVs.

Although the homodyne laser interferometer using the phase demodulation method is susceptible to noise, it is more suitable than the heterodyne laser interferometer for manufacturing a photonic integrated miniatured laser vibrometer due to its simpler configuration. In order to greatly enhance the performance of the homodyne laser interferometer in conditions with low SNRs, quadrature demodulation can be adopted in the design to recover the complete complex-domain photon signal. A schematic of quadrature demodulation is shown in Figure 2. An incoming signal beam can be split into an in-phase component (*I*) and a quadrature component (*Q*) through the beamsplitter in a 2-by-2 coupler. Similarly, a reference signal generated by a local oscillator (LO) laser can be split into two beams: one beam maintains its original phase for mixing with the in-phase component, while the other undergoes a (90°) phase shift to mix with the quadrature component. Therefore, quadrature demodulation can also be referred to as a (90°) mixing network. Four outputs from the (90°) mixing network can be expressed as

$$E_1 = \frac{1}{2}(E_{\text{sig}} + E_{\text{LO}}), \tag{1}$$

$$E_2 = \frac{1}{2}(E_{\text{sig}} - E_{\text{LO}}), \tag{2}$$

$$E_3 = \frac{1}{2}(E_{\text{sig}} + iE_{\text{LO}}), \tag{3}$$

$$E_4 = \frac{1}{2}(E_{\text{sig}} - iE_{\text{LO}}), \tag{4}$$

where $i = \sqrt{-1}$, and E_{sig} and E_{LO} are the signals of measurement and reference beams, respectively. Mixed signals can then be received by balanced PDs that can eliminate common-mode noise, yielding enhanced SNRs. Finally, a signal processing unit receives *I* and *Q* signals, and demodulates their amplitude and phase information, allowing for the precise detection of the input signal, which can be written as

$$I = R\sqrt{P_{\text{sig}}P_{\text{LO}}}\cos\left(\theta_{\text{sig}}(t) - \theta_{\text{LO}}(t)\right), \tag{5}$$

$$Q = R\sqrt{P_{\text{sig}}P_{\text{LO}}}\sin\left(\theta_{\text{sig}}(t) - \theta_{\text{LO}}(t)\right), \tag{6}$$

where R denotes the responsivity of PDs, P_{sig} and P_{LO} denote the amplitudes of the signals of measurement and reference beams, respectively, and θ_{sig} and θ_{LO} denote the phases of of the signals of measurement and reference beams, respectively.

Incorporating quadrature demodulation can significantly enhance the performance of demodulation by the following aspects. The first one is to enhance phase accuracy. The (90°) mixing network introduced above can produce two signals (*I* and *Q*) with a (90°) phase difference, thereby delivering comprehensive phase information. Compared to conventional amplitude-phase demodulation methods, such as a fringe counting method, the *I*/*Q* phase demodulation method uses digital

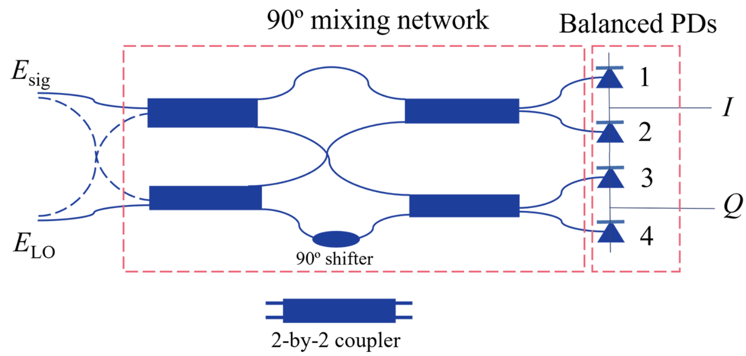

Fig. 2 Schematic of quadrature demodulation.

decoding, which can significantly improve the precision of measurement through subdivision. It ensures that the complete phase information can be accurately reconstructed by a complementary path when a signal path is disrupted by noise or partial distortion. The second one serves to resolve phase ambiguity. In a conventional single-frequency interferometer, phase measurement is typically limited to the range of $[0, 2\pi]$, which can lead to phase "folding" or "wrapping" beyond this range and cause ambiguity. The (90°) mixing network can resolve this issue by accurately computing the angle of two orthogonal signals, enabling accurate and continuous phase determination even beyond the range of $[0, 2\pi]$. Thus, the two orthogonal signals offer a more complete view of phase changes, expanding the dynamic range of measurement. This allows the interferometer to accurately measure the displacement or optical path difference variations over a wider range by digital decoding from a block of data. The last one is to reduce impacts from signal errors and noises. With two independent signal channels processed concurrently, specialized algorithms, such as trending detection and signal averaging, can minimize random noises and enhance the laser vibrometer's responsiveness to genuine signals. This data processing helps cancel the nonlinear errors induced by a variety of noise sources or environmental fluctuations.

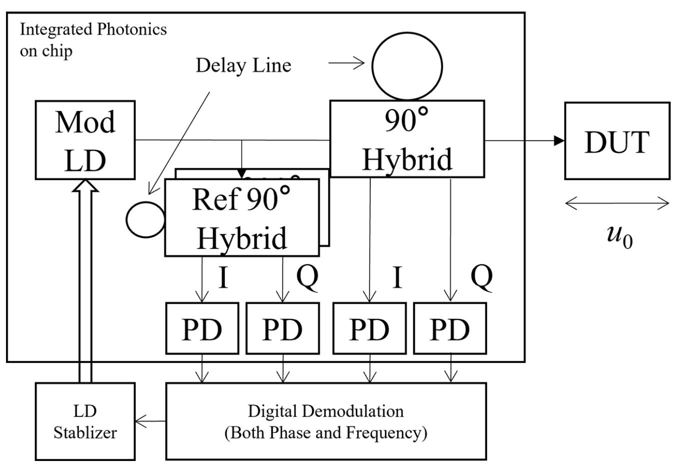

Fig. 3 Schematic of of the proposed chip-based high-precision laser vibrometer.

It is usually difficult to implement quadrature demodulation in a discrete optical device because it requires an accurate (90°) delay on one interference beam in the demodulation network. However, it is relatively easy for photonic integration as the modern lithography processing can accurately control the length of the waveguide. A schematic of the proposed chip-based high-precision laser vibrometer is shown in Figure 3. The laser vibrometer proposed in this work incorporates two or more sets of quadrature demodulation networks in the design. One of the quadrature demodulation networks serves as a main *I*/*Q* demodulator for detecting the interference signal between measurement and reference beams and enabling the extraction of the phase and amplitude information from the signal beam. A second quadrature demodulation network serves as a reference *I*/*Q* demodulator for capturing the phase and amplitude instability of the laser. The demodulated reference signal is used for a closed control loop to lock the laser wavelength, and thus ensure signal stability in the laser vibrometer. The reflection signal from the DUT is only fed into the first quadrature demodulation network, and is mixed with the local

LD source; *I*/*Q* signals are then decoded. The input signal of the second quadrature demodulation network is a split LD signal from the LD source after a delay line within the integrated photonic chip. This second quadrature demodulation network is used to catch the interference signal by slow laser center frequency drifting due to temperature change. The signal is considered as the common mode error and deducted by decoded results from the first quadrature demodulation network to retrieve an accurate signal from the DUT. As the delay line of the second quadrature demodulation network is co-printed with the delay line of the first quadrature demodulation network and the path lengths of the second quadrature demodulation network match with those of the first quadrature demodulation network, the common mode error can be removed by the proposed design. The novel laser vibrometer proposed in this work employs a fully digital demodulation approach to capture the comprehensive complex signal information. The reference *I*/*Q* demodulator stabilizes the frequency of the semiconductor laser through real-time feedback, reducing phase noise. This strategy allows the regular semiconductor laser with a prone-drifting center wavelength to achieve the performance level comparable to the conventional helium-neon gas laser. In addition, the modern semiconductor laser has a lower laser linewidth and can be easily integrated into a photonic chip.

Experimental Validation

Measurement Repeatability. Experimental validation of the measurement repeatability of the proposed laser vibrometer was conducted through comparisons among vibration responses from three independent measurements of a DUT. The experimental setups of measurement repeatability validation are shown in Figure 4, where the three DUTs were used for measurements with vibration frequencies much lower than, close to, and within the ultrasonic range, respectively. The laser vibrometer was attached to an adjustable frame in measurements to ensure that its laser beam was perpendicular to the surfaces of the DUTs and its laser spot was located at the centers of the DUTs. A signal generator was used to provide sinusoidal excitation to the DUTs. A speaker #1 shown in Figure 4a was used as the DUT that was under sinusoidal excitations with frequencies of 0.1 Hz, 1 Hz, 10 Hz, 100 Hz, and 1000 Hz, which were much lower than the ultrasonic range. A speaker #2 that was smaller than the speaker #1, as shown in Figure 4b, was used as the DUT that was under sinusoidal excitations with frequencies of 5000 Hz and 20,000 Hz, which were close to the ultrasonic range. An ultrasonic vibration source shown in Figure 4c was used as the DUT that was under sinusoidal excitation with a frequency of 1,000,000 Hz, which was within the ultrasonic range. For each excitation frequency, three independent tests were performed with the same data length. The sample results of the three DUTs are shown in Figures 5–7, respectively. One could see that the measured vibration responses from the three datasets for each excitation frequency had good agreement with each other in both the time and frequency domains. To further check the measurement repeatability, the peak values of the vibrations of the DUTs under various excitation frequencies were extracted from their frequency spectra and listed in Table 1, where the percentage differences among them were calculated by using each dataset #1 as a reference. One could see that the maximum difference was lower than 0.5%, meaning that the proposed laser vibrometer could measure vibrations in a wide frequency range with a high level of repeatability.

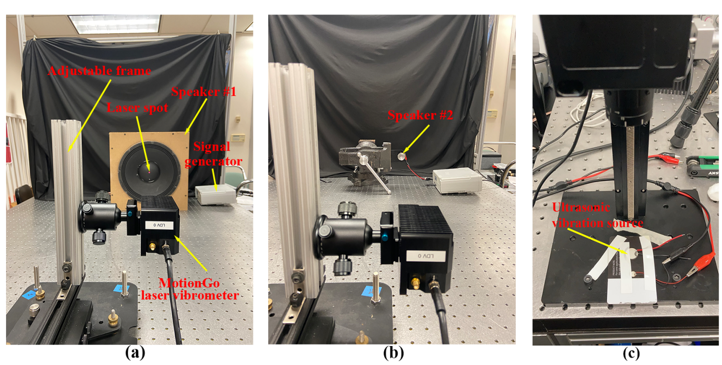

Fig. 4 Experimental setups of the measurement repeatability validation of the proposed laser vibrometer: (**a**) a speaker under excitation frequencies of 0.1 Hz–1000 Hz; (**b**) another speaker under excitation frequencies of 5000 Hz and 20,000 Hz; and (**c**) an ultrasonic vibration source under an excitation frequency of 1,000,000 Hz.

Measurement Accuracy. Experimental validation of the measurement accuracy of the proposed laser vibrometer was conducted through comparisons between vibration responses from the measurements of a DUT using two independent measure-

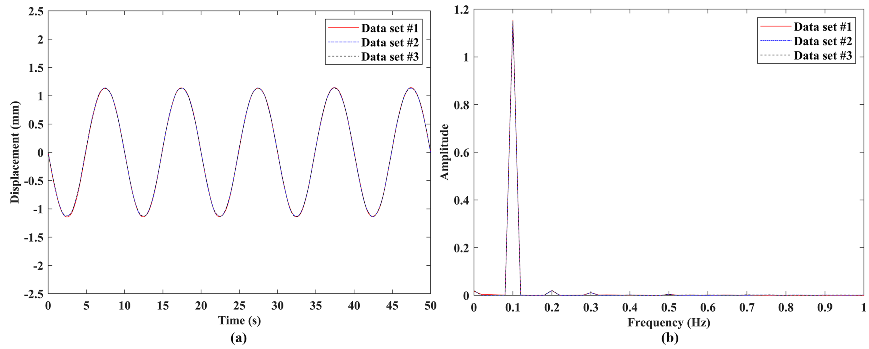

Fig. 5 Vibrations of the speaker #1 under sinusoidal excitation with a frequency of 0.1 Hz: responses from three independent datasets with the same length in the (**a**) time domain and (**b**) frequency domain.

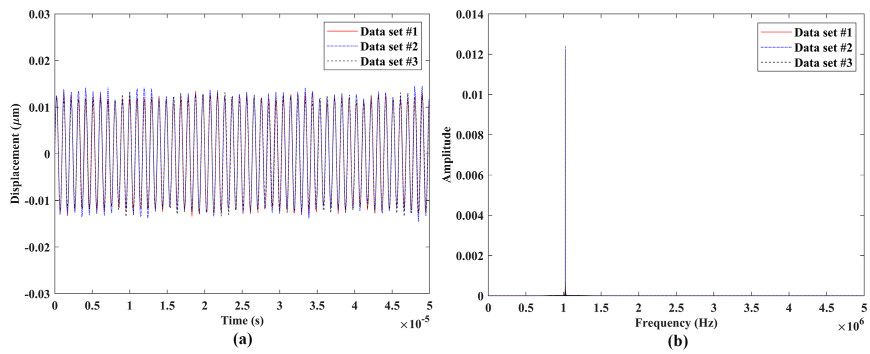

Fig. 6 Vibrations of the speaker #1 under sinusoidal excitation with a frequency of 20,000 Hz: responses from three independent datasets with the same length in the (**a**) time domain and (**b**) frequency domain.

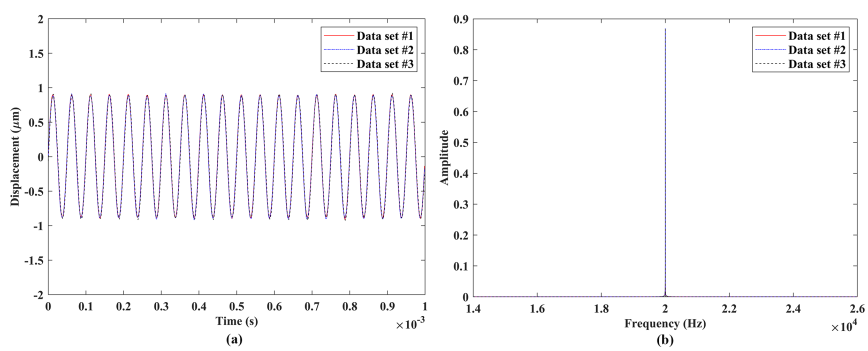

Fig. 7 Vibrations of the speaker #1 under sinusoidal excitation with a frequency of 1,000,000 Hz: responses from three independent datasets with the same length in the (**a**) time domain and (**b**) frequency domain.

ment systems; vibration response measured by a Polytec LDV (PSV-500) (Polytec GmbH, Waldbronn, Baden-Württemberg, Germany), as shown in Figure 8, was used as a reference. Speakers #1 and #2 were used in this work to provide vibrations with frequencies up to 5000 Hz, since the Polytec LDV used in this work had a limited maximum sampling rate and was not an LDV designed for measuring ultrasonic vibration. For each excitation frequency, the tests performed by the two measurement systems had the same data length. The sample results of the two DUTs were shown in Figures 9 and 10. Note that the responses measured by the proposed laser vibrometer were in terms of displacement, while those measured by the Polytec LDV were in terms of velocity. Therefore, velocity responses from the Polytec LDV were integrated to be displacement ones prior to comparison. One can see that the measured vibration responses from the two systems for each excitation frequency had good agreement with each other in both the time and frequency domains. To further check the measurement accuracy, the peak values of the vibrations of the DUTs under various excitation frequencies were ex-

Table 1 Peak values of vibrations of the DUTs under various excitation frequencies, where three independent datasets were measured for each excitation frequency and differences among them were calculated by using each dataset #1 as a reference (unit: μm).

DUT	Excitation frequency (Hz)	Dataset #1	Dataset #2	Dataset #3	Differences
Speaker #1	0.1	1154.4	1149.7	1149.3	0.4% & 0.4%
	1	116.1	116.2	116.3	0.1% & 0.2%
	10	75.3	75.2	75.4	0.1% & 0.1%
	100	30.3	30.3	30.3	0 & 0
	1000	4.9×10^{-1}	4.9×10^{-1}	4.9×10^{-1}	0 & 0
Speaker #2	5000	1.8×10^{-1}	1.8×10^{-1}	1.8×10^{-1}	0 & 0
	20,000	8.7×10^{-1}	8.7×10^{-1}	8.7×10^{-1}	0 & 0
Ultrasonic vibration source	1,000,000	1.2×10^{-2}	1.2×10^{-2}	1.2×10^{-2}	0 & 0

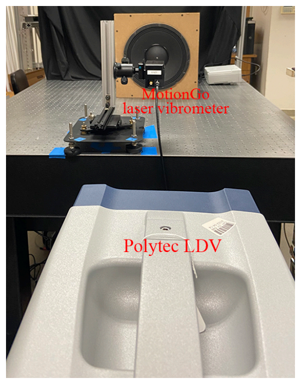

Fig. 8 Experimental setup of the measurement accuracy validation of the proposed laser vibrometer, where a Polytec LDV was used as a reference.

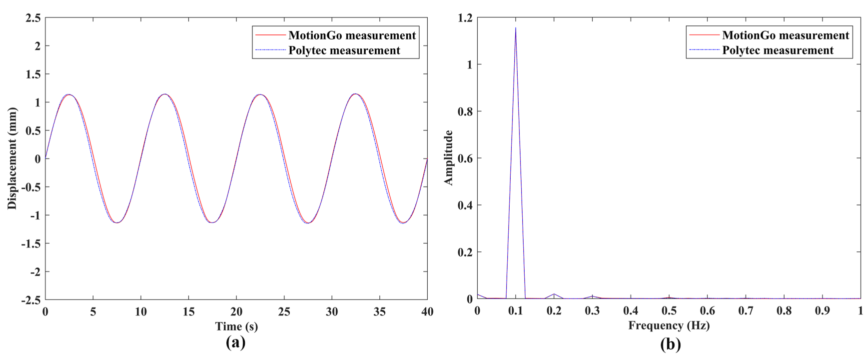

Fig. 9 Vibrations of the speaker #1 under sinusoidal excitation with a frequency of 0.1 Hz: responses from the two independent measurement systems with the same length in the (**a**) time domain and (**b**) frequency domain.

tracted from their frequency spectra and listed in Table 2. One could see that the maximum difference was lower than 1%, meaning that the proposed laser vibrometer could measure vibrations in0 a wide frequency range with a high level of accuracy.

Robustness to Test Surface Conditions. This section aimed to assess the performance of the proposed laser vibrometer for different test surface conditions, where the SNR was used as an indicator. The experimental setup is shown in Figure 11, where the left subfigure was the speaker #1 with a piece of reflective tape on its surface and the right subfigure was the speaker #1 with its natural surface. It could be seen that the natural surface of the speaker #1 was dark and rough, meaning that it had weak reflection. For a conventional LDV without a signal enhancement technique, attaching a reflective tape on the test structure surface was an important and necessary step in the test preparation stage. A signal enhancement technique,

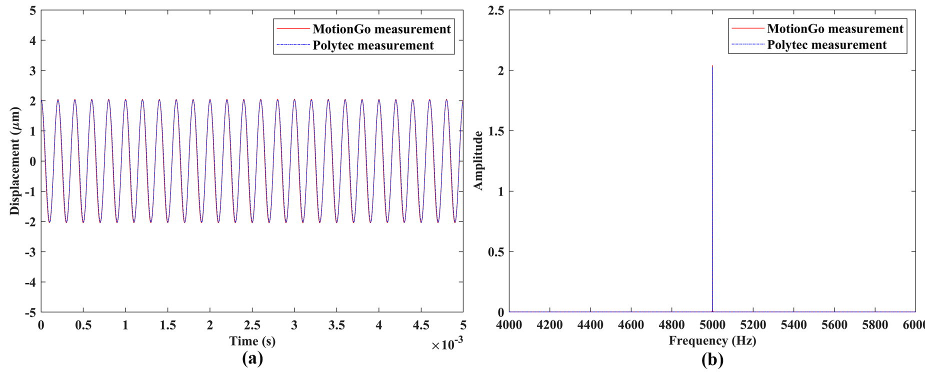

Fig. 10 Vibrations of the speaker #2 under sinusoidal excitation with a frequency of 5000 Hz: responses from the two independent measurement systems with the same length in the (**a**) time domain and (**b**) frequency domain.

Table 2 Peak values of vibrations of the DUTs under various excitation frequencies, where vibration responses were measured for each excitation frequency using the two independent measurement systems and differences among them were calculated by using each data from the Polytec LDV as a reference (unit: μm).

DUT	Excitation Frequency (Hz)	Polytec Measurement	MotionGo Measurement	Differences
Speaker #1	0.1	1157.99	1157.97	¡¡0.01%
	1	600.95	595.17	0.96%
	10	75.50	74.97	0.70%
	100	44.67	44.61	0.13%
	1000	4.97×10^{-1}	4.95×10^{-1}	0.40%
Speaker #2	5000	2.03	2.04	0.49%

such as the QTec technology developed by Polytec, usually used multiple channels, while the laser vibrometer proposed in this work was based on a single-channel detection. For fair comparison purposes, a conventional Polytec LDV without the QTec technology signal enhancement was used in this comparison. Vibration responses of the speaker #1 under sinusoidal excitations with frequencies of 10 Hz and 1000 Hz, measured by the Polytec LDV, which was a conventional model without the QTec technology, were shown in Figures 12a and 13a, respectively. One could see that the SNRs of the responses slightly decreased from 53.69 to 51.59 for the case of 10 Hz excitation, and significantly decreased from 11.42 to 7.46 for the case of 1000 Hz excitation, when removing the reflective tape. Vibration responses of the speaker #1 under sinusoidal excitations with frequencies of 10 Hz and 1000 Hz, measured by the proposed laser vibrometer, are shown in Figures 12b and 13b, respectively. The SNRs of the responses remained approximately constant for enhanced and natural surfaces, meaning that the proposed laser vibrometer had a good robustness to the test surface conditions. Note that the SNR results from the two measurement systems were not compared to each other, as they had different measurement conditions, such as measurement distances and optical diameters.

Conclusion

This work proposes a novel chip-based high-precision laser vibrometer that can directly measure the vibration displacement of a structure through the phase demodulation method. The feasibility for the productization and the features for the vibration measurement of the proposed miniatured laser vibrometer are discussed in this work. Some conclusions are listed as follows:

1. The laser vibrometer proposed in this work incorporates two or more sets of quadrature demodulation networks in the design. One quadrature demodulation network serves as a main I/Q demodulator for signal measurement. A reference quadrature demodulation network can capture the phase and amplitude instability of the laser. Correlation between the signals from the first and second quadrature networks can be computed to mitigate signal interference caused by ghost reflectance or scattering signals. A third quadrature demodulation network set with a distinct reference arm delay line length can be included to further compensate the temperature effect by capturing temperature or environmental variations that impact its delay line.

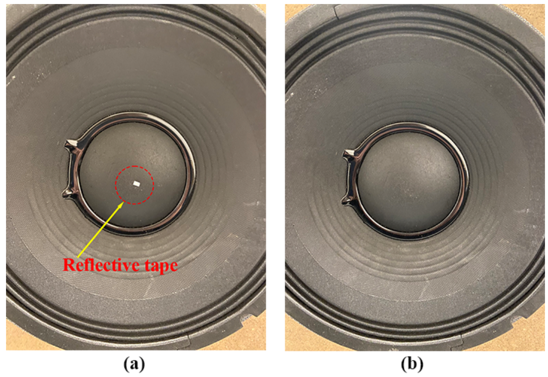

Fig. 11 Experimental setup for assessing the robustness of the proposed laser vibrometer to test surface conditions using the speaker #1 with (**a**) a surface enhanced by a reflective tape, and (**b**) a natural surface.

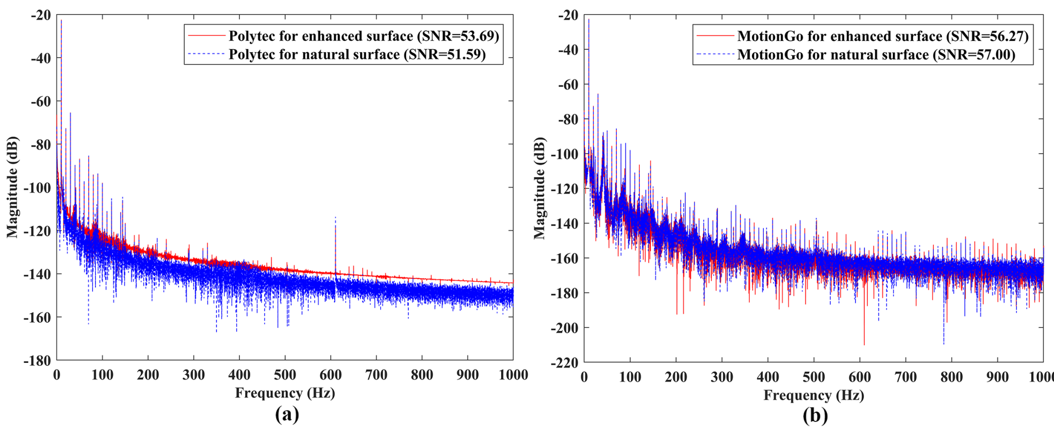

Fig. 12 SNRs of measured responses of the speaker #1 with enhanced and natural surfaces under sinusoidal excitation with a frequency of 10 Hz using (**a**) the Polytec LDV, and (**b**) the proposed laser vibrometer.

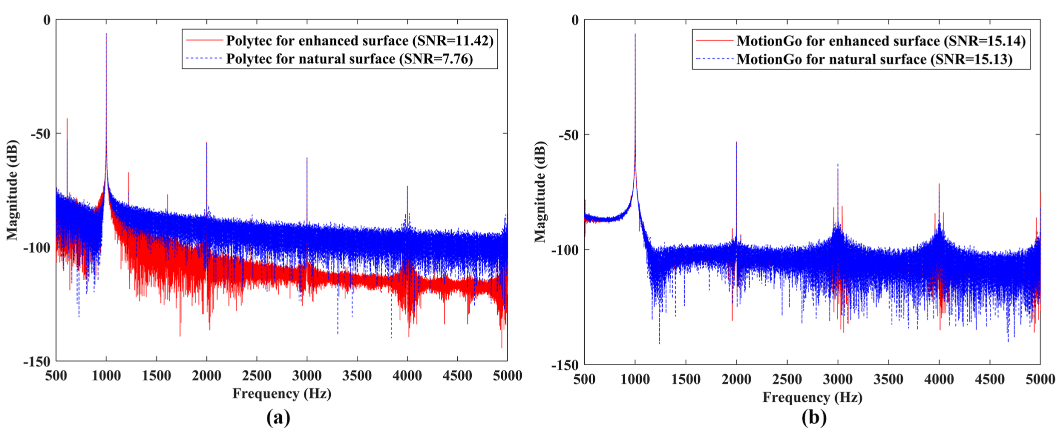

Fig. 13 SNRs of measured responses of the speaker #1 with enhanced and natural surfaces under sinusoidal excitation with a frequency of 1000 Hz using (**a**) the Polytec LDV, and (**b**) the proposed laser vibrometer.

2. Experimental validation of the measurement repeatability of the proposed laser vibrometer was conducted through comparisons among the vibration responses from the three independent measurements of the DUTs under sinusoidal excitations with frequencies from 0.1 Hz to 1,000,000 Hz. The maximum difference among measurements is lower than 0.5%, meaning that the proposed laser vibrometer can measure vibrations in a wide frequency range with a high level of repeatability.

3. Experimental validation of the measurement accuracy of the proposed laser vibrometer was conducted through comparisons between vibration responses from measurements of the DUTs using the proposed laser vibrometer and a Polytec LDV. The maximum difference between the results from the two measurement systems was lower than 1%, meaning that the proposed laser vibrometer could measure vibrations in a wide frequency range with a high level of accuracy.
4. SNRs of responses measured by the proposed laser vibrometer could remain approximately constant for surfaces with and without reflective tapes, meaning that it had better robustness to test surface conditions than a conventional LDV.

Acknowledgments This research was funded by the Maryland Industrial Partnerships Program through the grant number 7207 and the National Science Foundation through the grant number 1763024.

References

1. Lyu, L., Yuan, K., and Zhu, W. "A novel demodulation method with a reference signal for operational modal analysis and baseline-free damage detection of a beam under random excitation". *Journal of Sound and Vibration*, 571:118068 (2024)
2. Yuan, K. and Zhu, W. "In-plane operating deflection shape measurement of an aluminum plate using a three-dimensional continuously scanning laser doppler vibrometer system". *Experimental Mechanics*, pages 667–676 (2022)
3. Rezaei, D. and Taheri, F. "A novel application of a laser doppler vibrometer in a health monitoring system". *Journal of Mechanics of Materials and Structures*, 5(2):289–304 (2010)
4. Yuan, K. and Zhu, W. "A novel mirror-assisted method for full-field vibration measurement of a hollow cylinder using a three-dimensional continuously scanning laser doppler vibrometer system". *Mechanical Systems and Signal Processing*, 216:111428 (2024)
5. Nassif, H.H., Gindy, M., and Davis, J. "Comparison of laser doppler vibrometer with contact sensors for monitoring bridge deflection and vibration". *Ndt & E International*, 38(3):213–218 (2005)
6. Yu, T., Tang, Q., and Vinayaka, S. "Identifying structural properties of a steel railway bridge for structural health monitoring using laser doppler vibrometry". *Automation in Construction*, 160:105320 (2024)
7. Roozen, N.B., Labelle, L., Rychtáriková, M., and Glorieux, C. "Determining radiated sound power of building structures by means of laser doppler vibrometry". *Journal of Sound and Vibration*, 346:81–99 (2015)
8. Huang, Z., Xie, M., Chen, C., Du, Y., and Zhao, J. "Engineering application of a safety-state evaluation model for hidden frame-supported glass curtain walls based on remote vibration". *Journal of Building Engineering*, 26:100915 (2019)
9. Yuan, K. and Zhu, W. "Identification of modal parameters of a model turbine blade with a curved surface under random excitation with a three-dimensional continuously scanning laser doppler vibrometer system". *Measurement*, 214:112759 (2023)
10. Zabihi, A., Aghdasi, F., Ellouzi, C., Singh, N.K., Jha, R., and Shen, C. "Non-contact wind turbine blade crack detection using laser doppler vibrometers". *Energies*, 17(9):2165 (2024)
11. Yuan, K. and Zhu, W. "Modeling of welded joints in a pyramidal truss sandwich panel using beam and shell finite elements". *Journal of Vibration and Acoustics*, 143(4):041002 (2021)
12. Hameury, C., Ferrari, G., Franchini, G., and Amabili, M. "An experimental approach to multi-input multi-output nonlinear active vibration control of a clamped sandwich beam". *Mechanical Systems and Signal Processing*, 216:111496 (2024)
13. Garg, P., Moreu, F., Ozdagli, A., Taha, M.R., and Mascareñas, D. "Noncontact dynamic displacement measurement of structures using a moving laser doppler vibrometer". *Journal of Bridge Engineering*, 24(9):04019089 (2019)
14. Garg, P., Nasimi, R., Ozdagli, A., Zhang, S., Mascarenas, D.D.L., Reda Taha, M., and Moreu, F. "Measuring transverse displacements using unmanned aerial systems laser doppler vibrometer (uas-ldv): Development and field validation". *Sensors*, 20(21):6051 (2020)
15. Bertini, L., Neri, P., Santus, C., and Guglielmo, A. "Automated experimental modal analysis of bladed wheels with an anthropomorphic robotic station". *Experimental Mechanics*, 57:273–285 (2017)
16. Margerit, P., Gobin, T., Lebée, A., and Caron, J.F. "The robotized laser doppler vibrometer: On the use of an industrial robot arm to perform 3d full-field velocity measurements". *Optics and Lasers in Engineering*, 137:106363 (2021)
17. Ahmed, H., Mohsin, A., Hong, S.C., Lee, J.R., and Ihn, J.B. "Robotic laser sensing and laser mirror excitation for pulse-echo scanning inspection of fixed composite structures with non-planar geometries". *Measurement*, 176:109109 (2021)
18. Brethee, K.F., Uwayed, A.N., and Alden Qwam, A.Y. "A novel index for vibration-based damage detection technique in laminated composite plates under forced vibrations: Experimental study". *Structural Health Monitoring*, 22(5):3109–3125 (2023)
19. Li, Y., Verstuyft, S., Yurtsever, G., Keyvaninia, S., Roelkens, G., Van Thourhout, D., and Baets, R. "Heterodyne laser doppler vibrometers integrated on silicon-on-insulator based on serrodyne thermo-optic frequency shifters". *Applied optics*, 52(10):2145–2152 (2013)
20. Li, Y. and Baets, R. "Homodyne laser doppler vibrometer on silicon-on-insulator with integrated 90 degree optical hybrids". *Optics Express*, 21(11):13342–13350 (2013)
21. Li, Y., Dieussaert, E., and Baets, R. "Miniaturization of laser doppler vibrometers—a review". *Sensors*, 22(13):4735 (2022)
22. Ramasubramanian, K. and Instruments, T. "Using a complex-baseband architecture in fmcw radar systems". *Texas Instruments*, 19 (2017)
23. Nguyen, T.H., Scalart, P., Gay, M., Bramerie, L., Peucheret, C., Gomez-Agis, F., Sentieys, O., Simon, J.C., and Joindot, M. "New metric for iq imbalance compensation in optical qpsk coherent systems". *Photonic Network Communications*, 36:326–337 (2018)